

Electronic Supplementary Information

Model, Self-assembly Structures, and Phase Diagram of Soft Janus Particles

Zhan-Wei Li,[†] Zhong-Yuan Lu,[‡] Zhao-Yan Sun,^{*,†} and Li-Jia An[†]

*State Key Laboratory of Polymer Physics and Chemistry, Changchun Institute of Applied
Chemistry, Chinese Academy of Sciences, Changchun 130022, China, and Institute of Theoretical
Chemistry, State Key Laboratory of Theoretical and Computational Chemistry, Jilin University,
Changchun 130023, China*

E-mail: zysun@ciac.jl.cn

KEYWORDS: American Chemical Society, L^AT_EX

*To whom correspondence should be addressed

[†]Changchun Institute of Applied Chemistry

[‡]Jilin University

Table S1: The corresponding relation between the strength of attraction α_{11}^A and the range of attraction δ or the adhesion energy G when $\alpha_{11}^R = 396$. In the simulations, increasing α_{11}^A corresponds to the increase of the adhesion energy G in a reasonable range from $2.00 k_B T$ to $25.00 k_B T$, which may represent hydrophobic or hydrogen bond interactions between the patches, and can also be tuned by altering salt concentration, pH, or temperature in experiments. The range of attraction δ will also gradually increase because of the deformability of soft Janus particles. The parameters α_{11}^R , α_{11}^A , and δ are given in reduced units.

$G [k_B T]$	α_{11}^R	α_{11}^A	δ
2.00	396	88	0.10
4.13	396	132	0.14
6.77	396	176	0.18
9.82	396	220	0.22
13.20	396	264	0.25
16.84	396	308	0.28
20.71	396	352	0.31
24.75	396	396	0.33

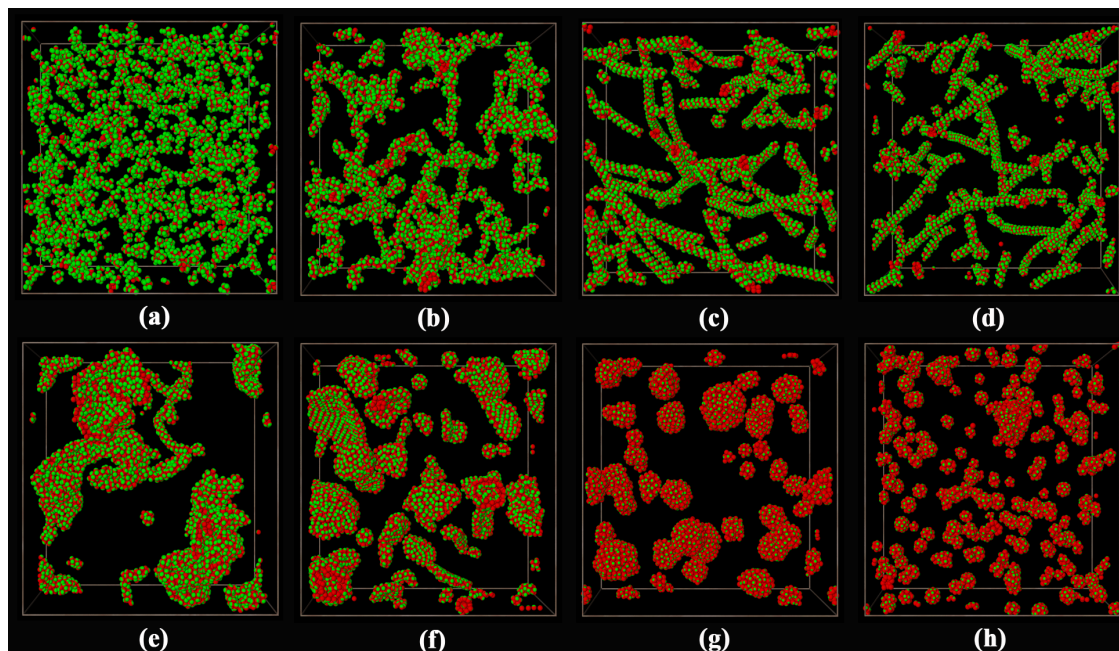


Figure S1: Typical self-assembled structures for larger system size of 98304 particles in a $32 \times 32 \times 32$ cubic box. (a)-(h) represent the star symbols b-g, j, and k in Fig. 2a, respectively. For the sake of clarity, we only show Janus solute particles in these systems.

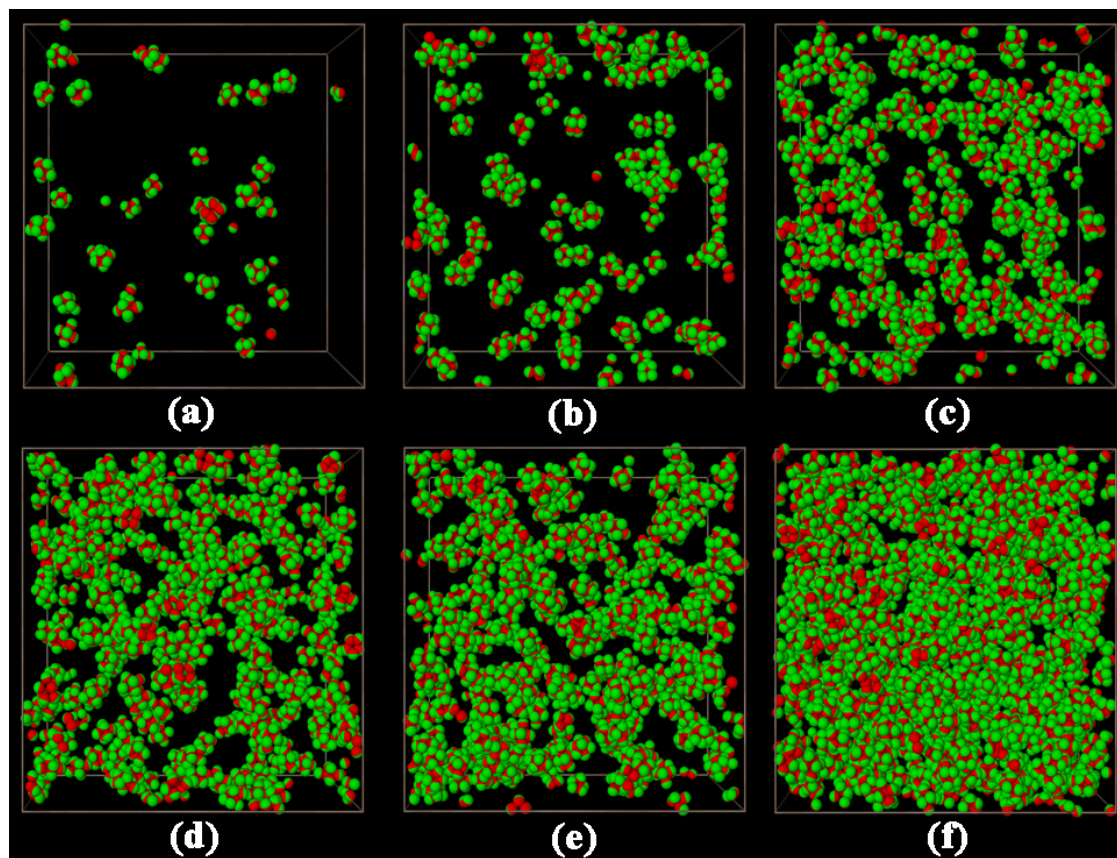


Figure S2: The effect of the concentration of Janus particles ϕ on micelles marked by star symbol b in Fig. 2a. (a) $\phi = 1\%$, (b) $\phi = 3\%$, (c) $\phi = 7\%$, (d) $\phi = 9\%$, (e) $\phi = 10\%$, (f) $\phi = 20\%$.

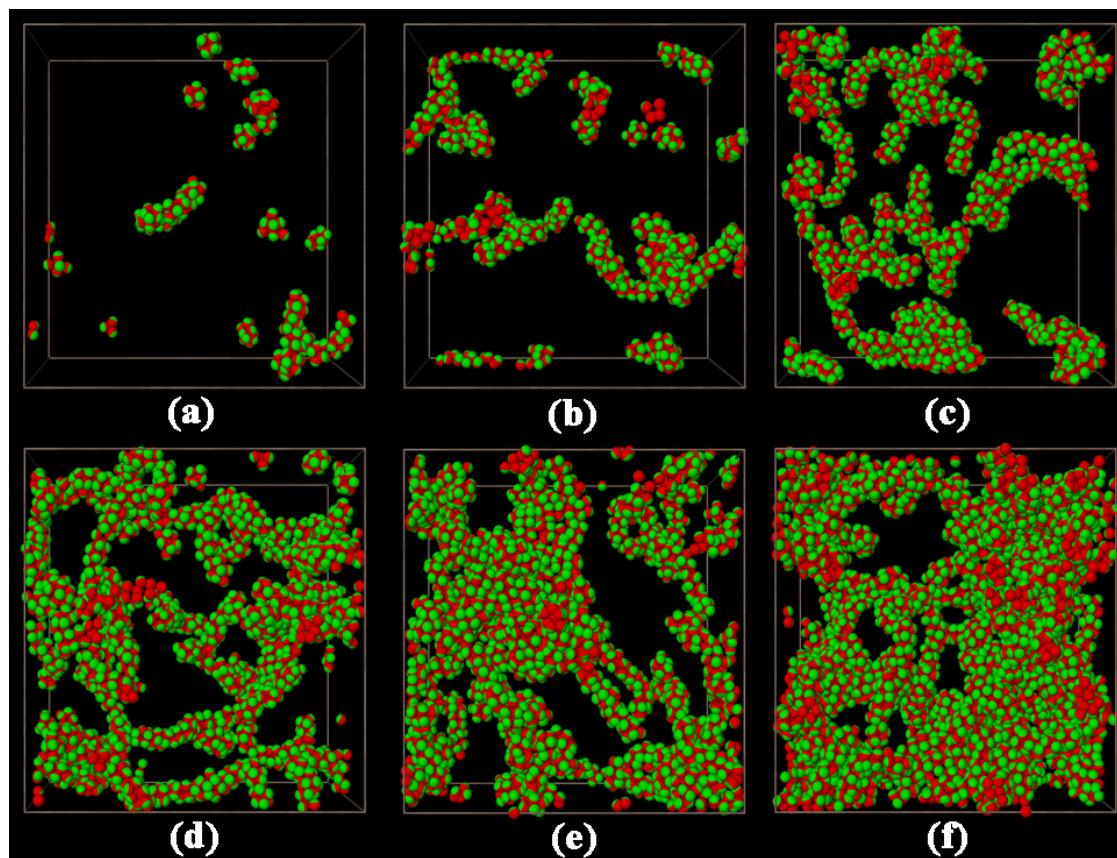


Figure S3: The effect of the concentration of Janus particles ϕ on wormlike strings marked by star symbol c in Fig. 2a. (a) $\phi = 1\%$, (b) $\phi = 3\%$, (c) $\phi = 7\%$, (d) $\phi = 9\%$, (e) $\phi = 10\%$, (f) $\phi = 20\%$.

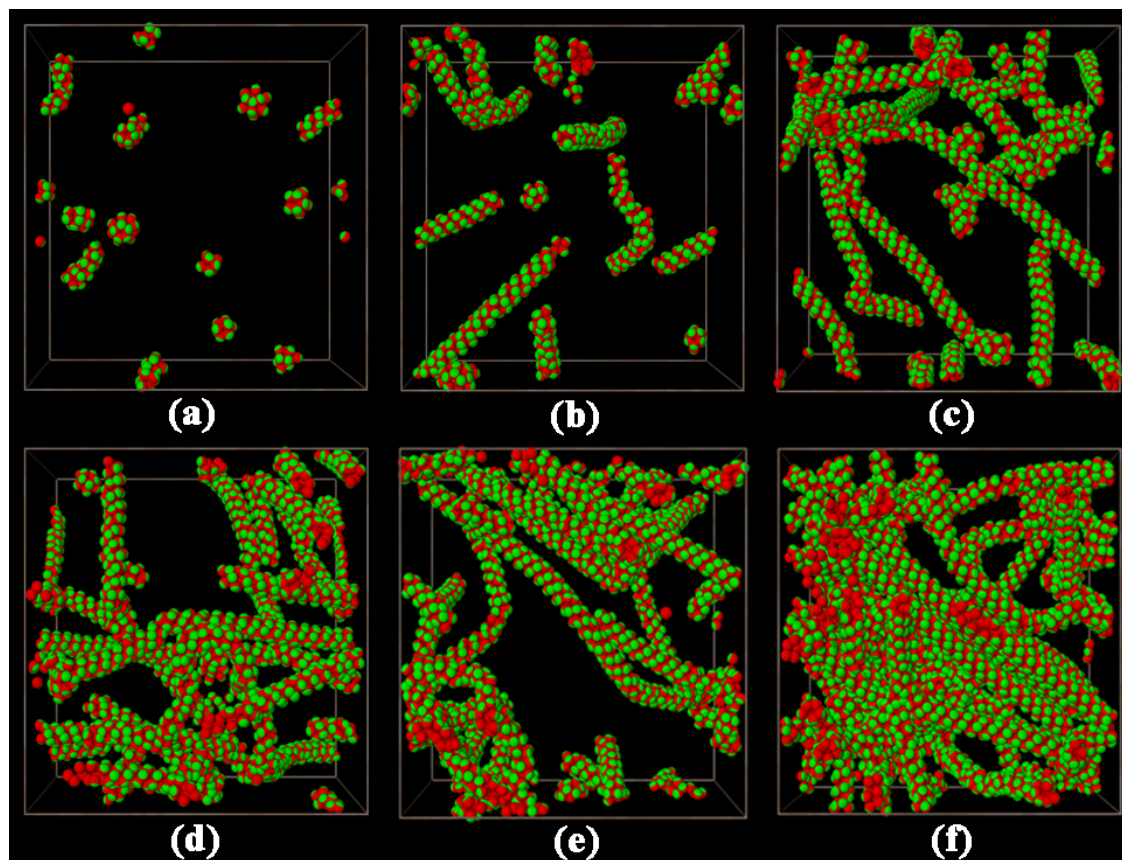


Figure S4: The effect of the concentration of Janus particles ϕ on double helices marked by star symbol d in Fig. 2a. (a) $\phi = 1\%$, (b) $\phi = 3\%$, (c) $\phi = 7\%$, (d) $\phi = 9\%$, (e) $\phi = 10\%$, (f) $\phi = 20\%$.

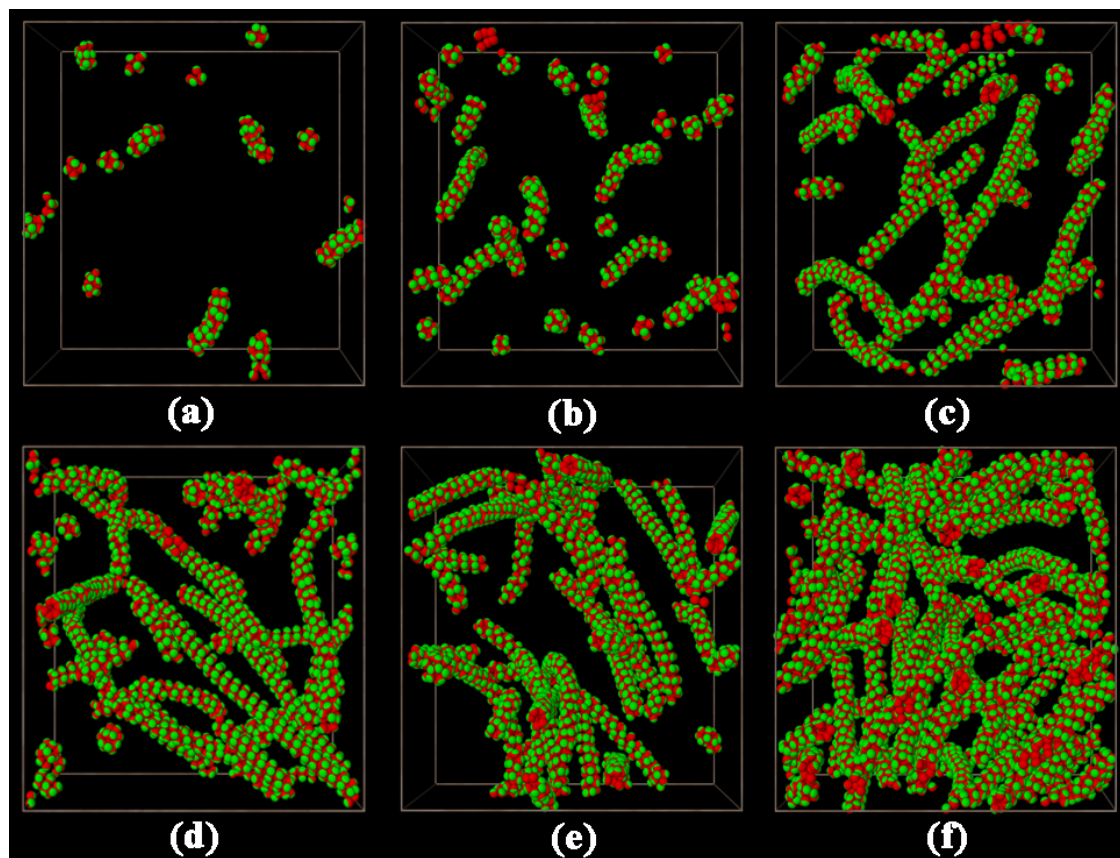


Figure S5: The effect of the concentration of Janus particles ϕ on single helices marked by star symbol e in Fig. 2a. (a) $\phi = 1\%$, (b) $\phi = 3\%$, (c) $\phi = 7\%$, (d) $\phi = 9\%$, (e) $\phi = 10\%$, (f) $\phi = 20\%$.

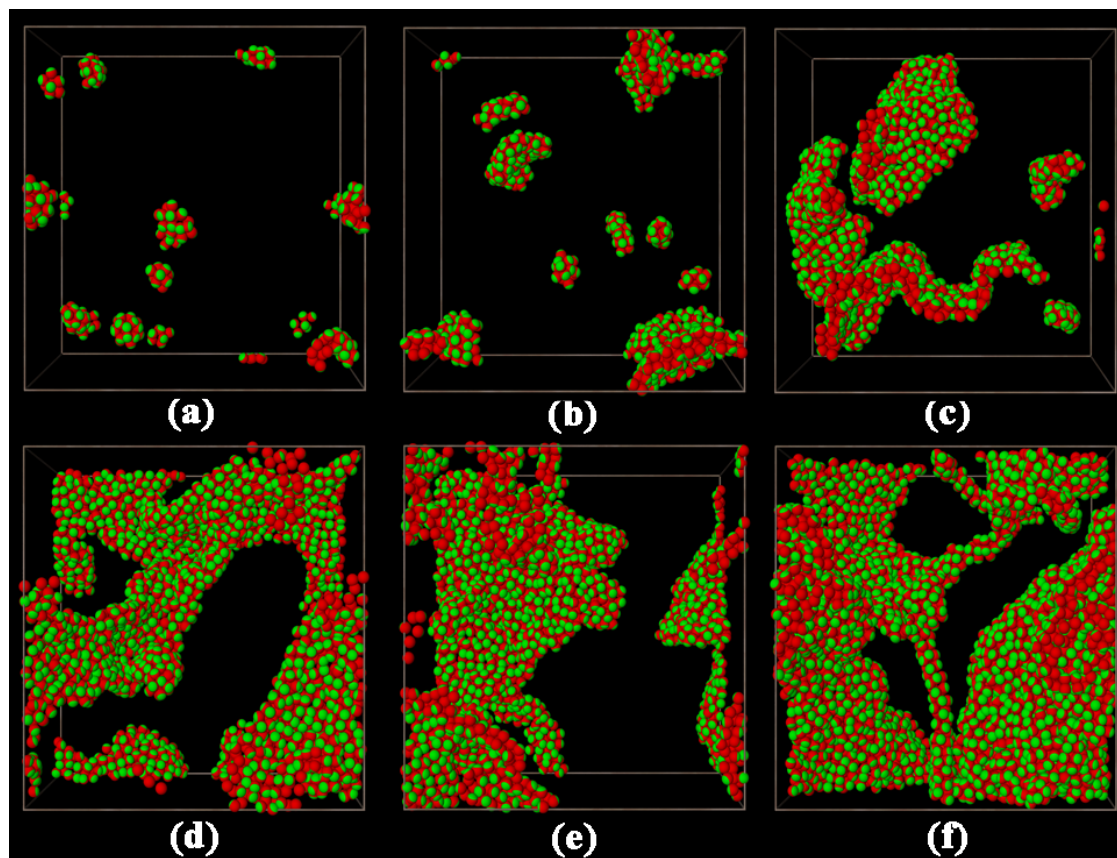


Figure S6: The effect of the concentration of Janus particles ϕ on bilayers marked by star symbol f in Fig. 2a. (a) $\phi = 1\%$, (b) $\phi = 3\%$, (c) $\phi = 7\%$, (d) $\phi = 9\%$, (e) $\phi = 10\%$, (f) $\phi = 20\%$.

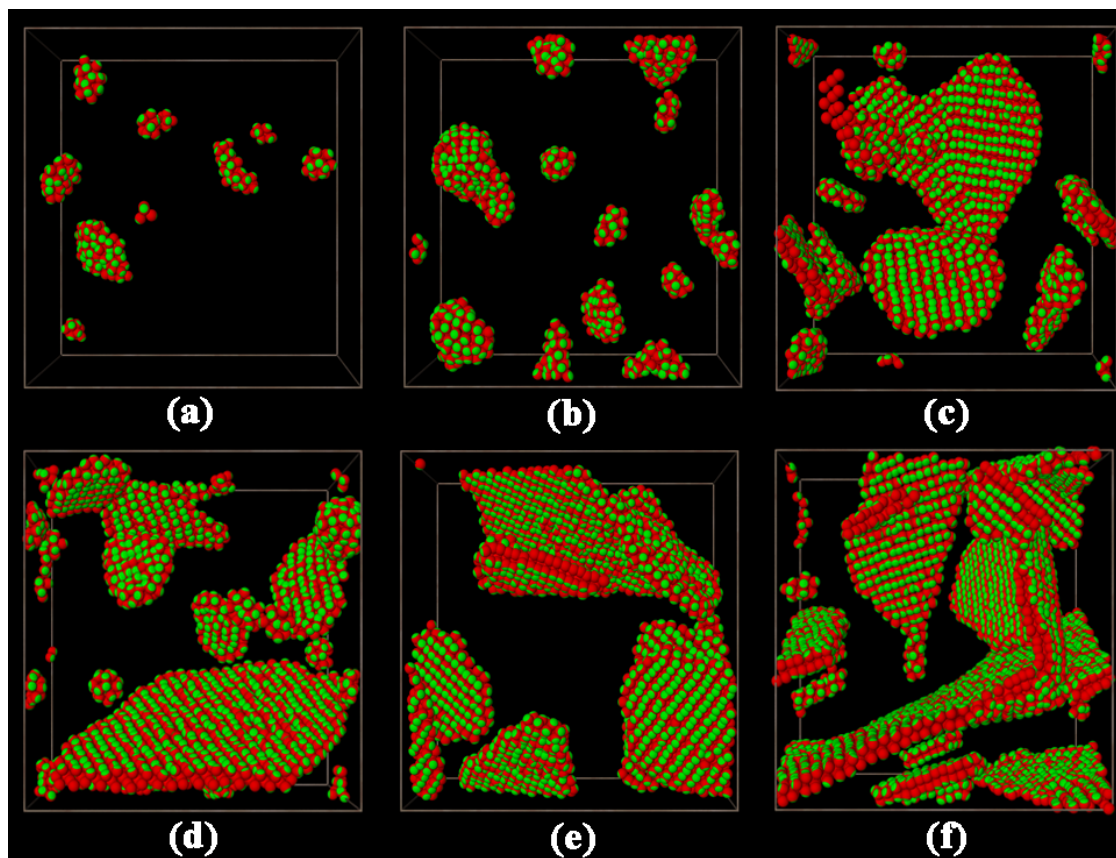


Figure S7: The effect of the concentration of Janus particles ϕ on tetragonal bilayers marked by star symbol g in Fig. 2a. (a) $\phi = 1\%$, (b) $\phi = 3\%$, (c) $\phi = 7\%$, (d) $\phi = 9\%$, (e) $\phi = 10\%$, (f) $\phi = 20\%$.

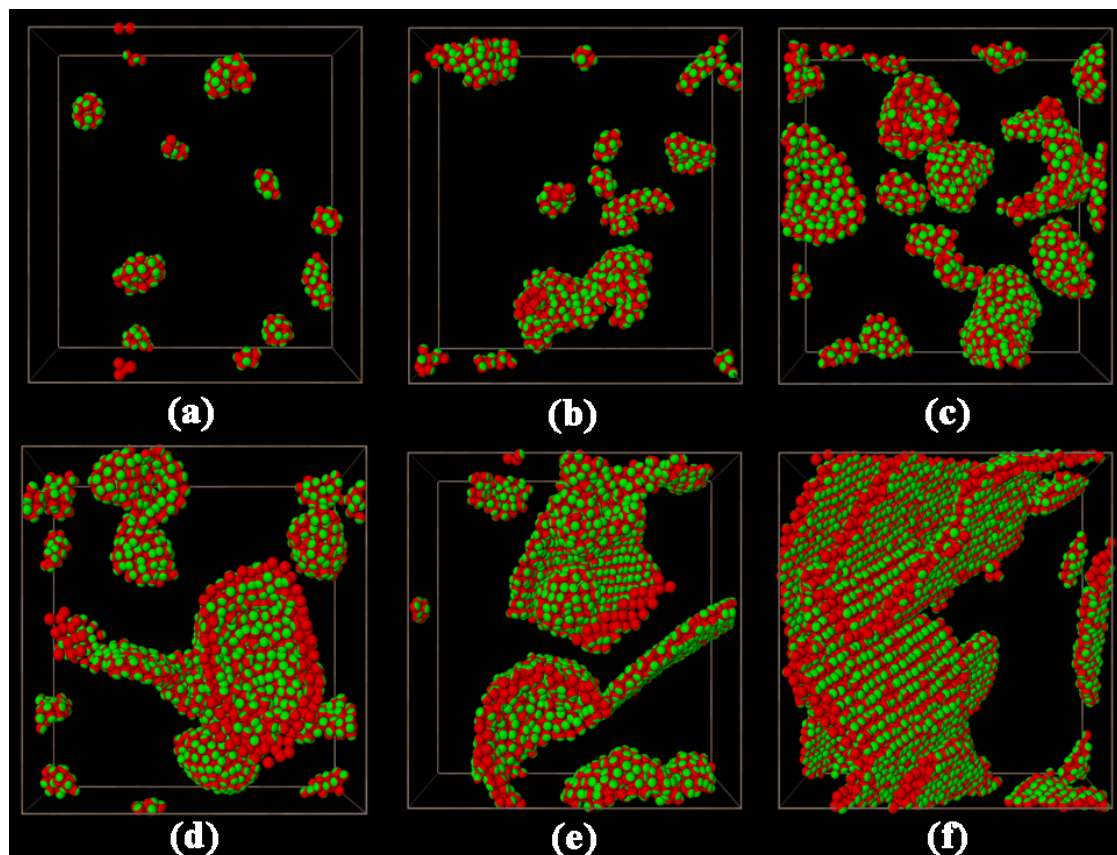


Figure S8: The effect of the concentration of Janus particles ϕ on coexisting phases of vesicles and bilayers marked by star symbol h in Fig. 2a. (a) $\phi = 1\%$, (b) $\phi = 3\%$, (c) $\phi = 7\%$, (d) $\phi = 9\%$, (e) $\phi = 10\%$, (f) $\phi = 20\%$.

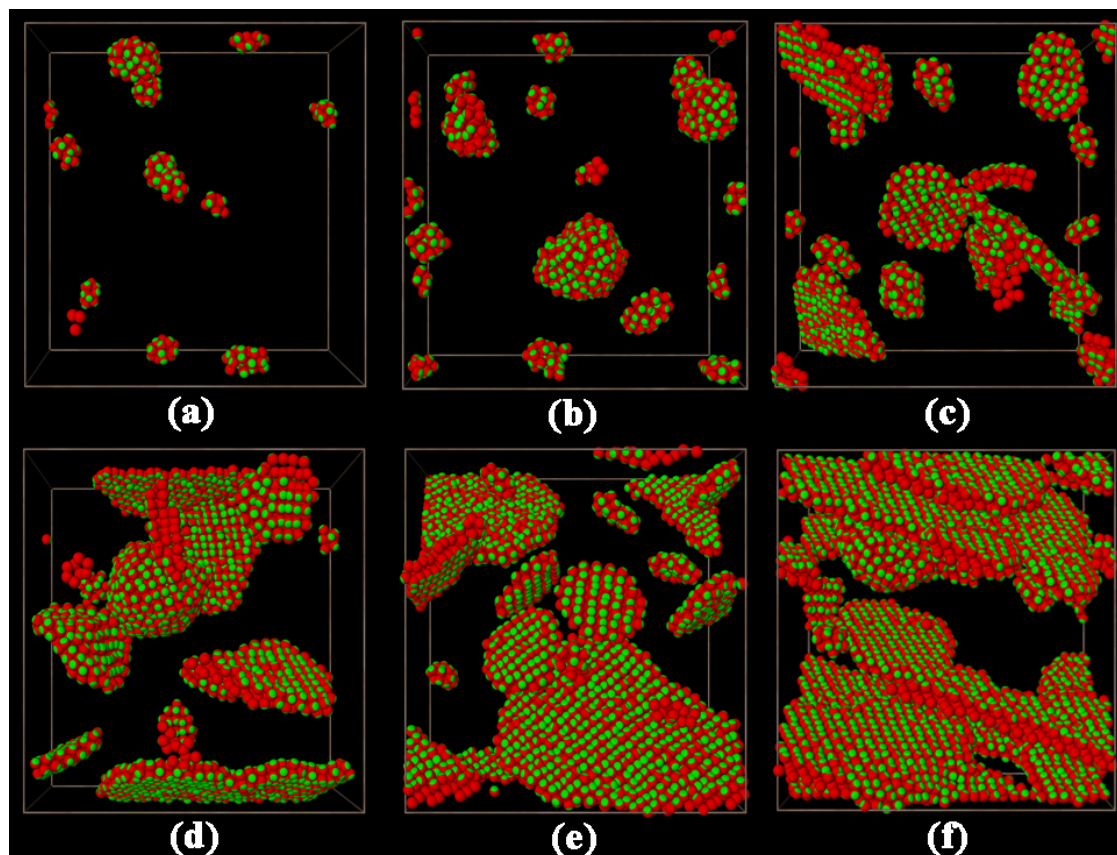


Figure S9: The effect of the concentration of Janus particles ϕ on coexisting phases of vesicles and tetragonal bilayers marked by star symbol i in Fig. 2a. (a) $\phi = 1%$, (b) $\phi = 3%$, (c) $\phi = 7%$, (d) $\phi = 9%$, (e) $\phi = 10%$, (f) $\phi = 20%$.

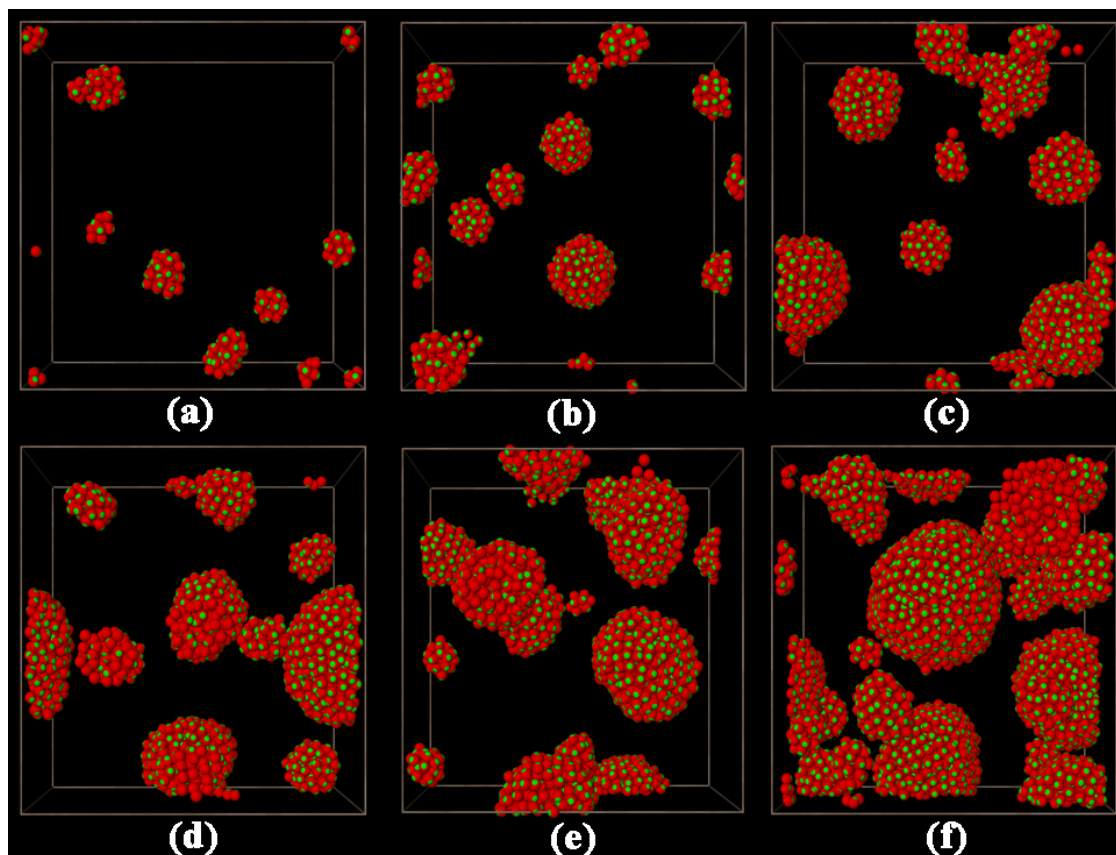


Figure S10: The effect of the concentration of Janus particles ϕ on complex supermicelles marked by star symbol j in Fig. 2a. (a) $\phi = 1\%$, (b) $\phi = 3\%$, (c) $\phi = 7\%$, (d) $\phi = 9\%$, (e) $\phi = 10\%$, (f) $\phi = 20\%$.

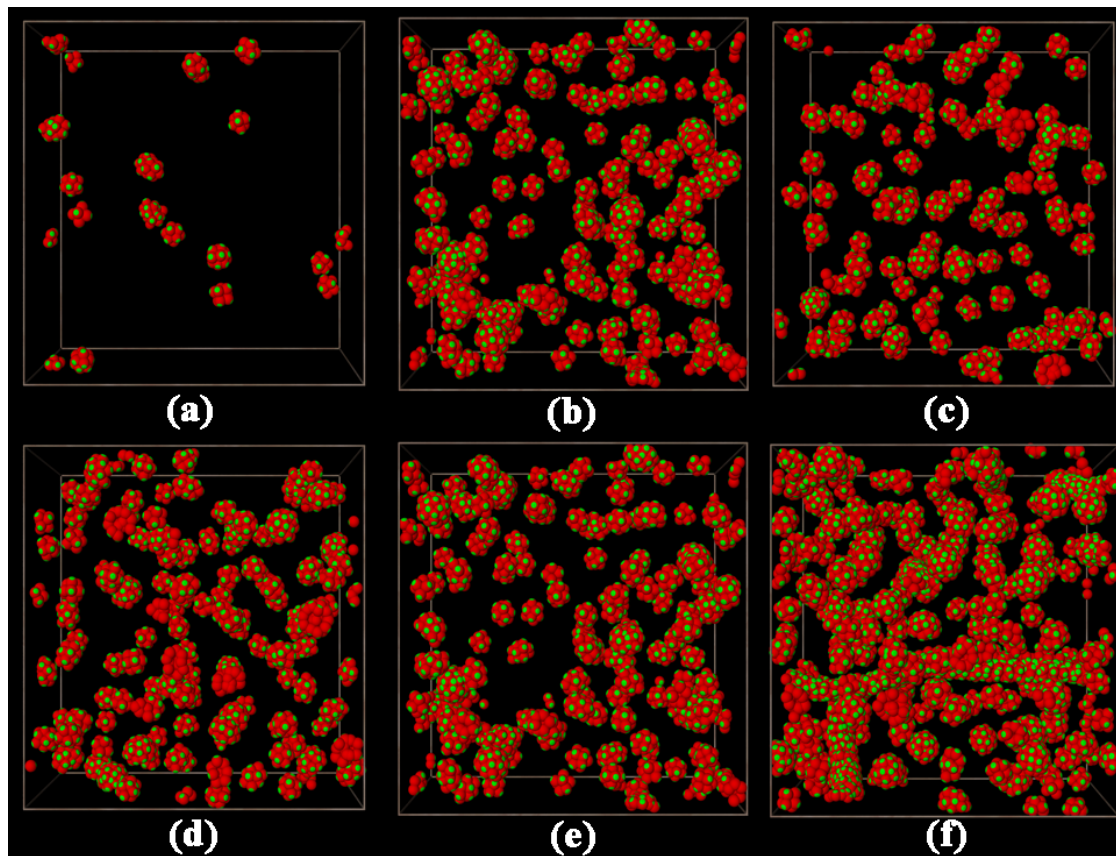


Figure S11: The effect of the concentration of Janus particles ϕ on micelles marked by star symbol k in Fig. 2a. (a) $\phi = 1\%$, (b) $\phi = 3\%$, (c) $\phi = 7\%$, (d) $\phi = 9\%$, (e) $\phi = 10\%$, (f) $\phi = 20\%$.

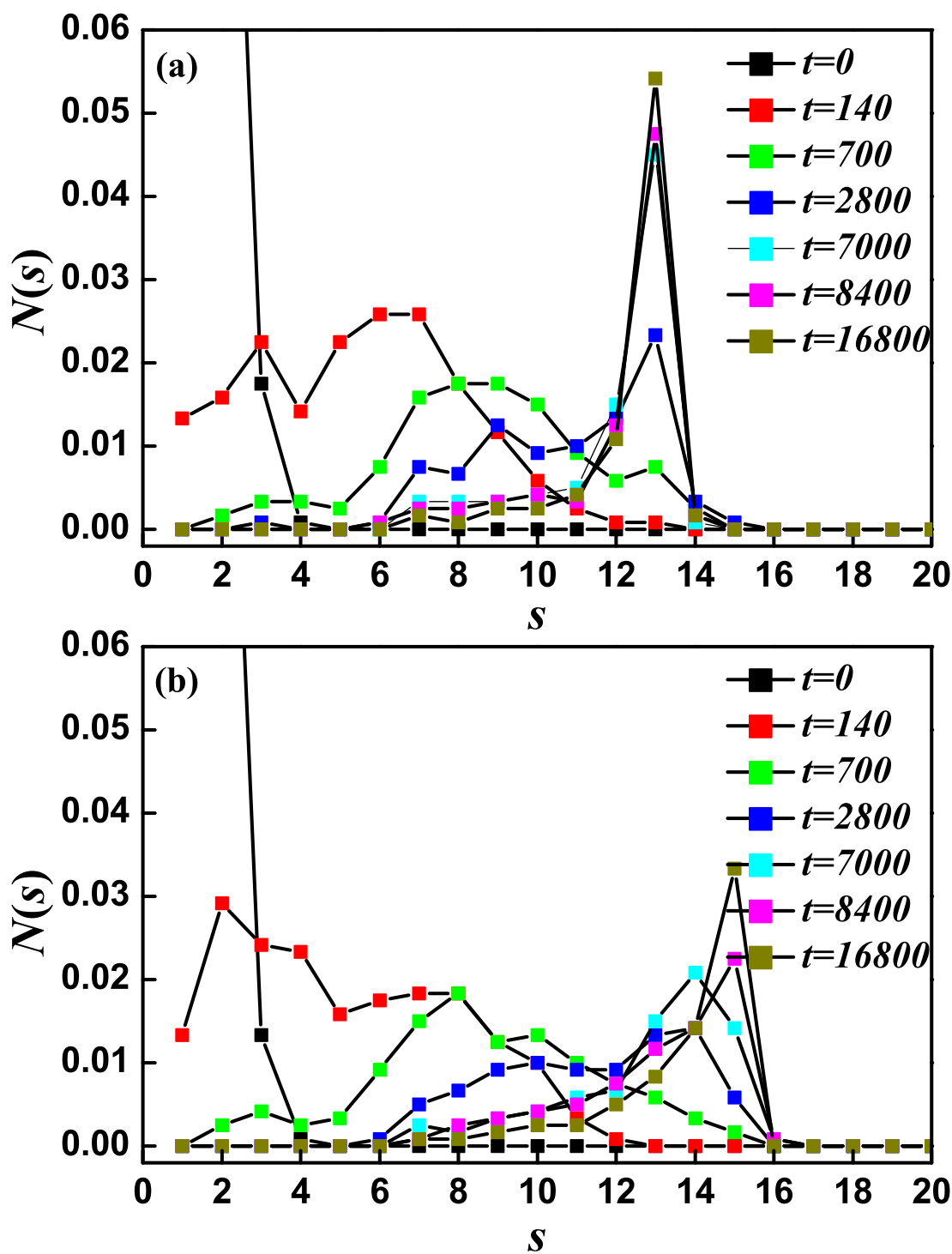


Figure S12: Time evolution of the distribution $N(s)$ of the number of contacts between attractive patches per Janus particle s for (a) double helices marked by star symbol d in Fig. 2a and (b) single helices marked by star symbol e in Fig. 2a.

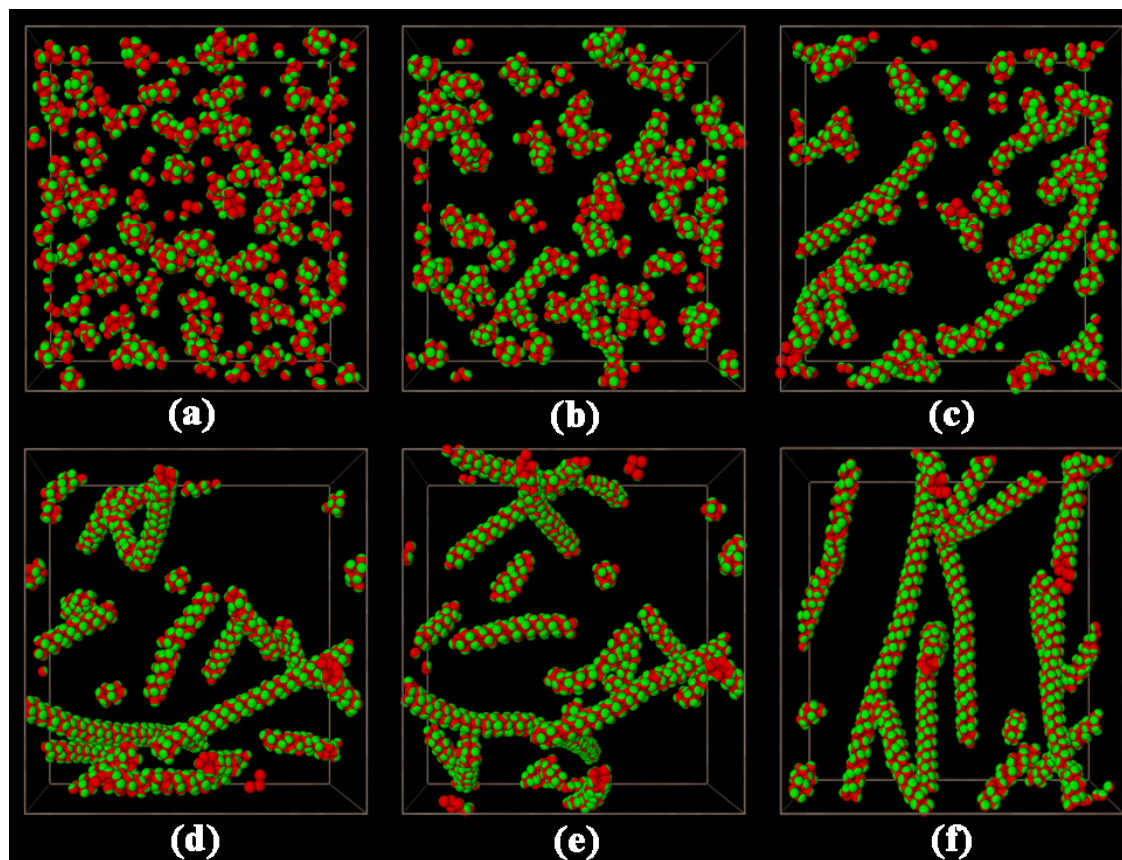


Figure S13: Snapshots taken from the formation process of double helices marked by star symbol d in Fig. 2a, after (a) 140, (b) 700, (c) 2800, (d) 7000, (e) 8400, (f) 16800 time units of simulation.

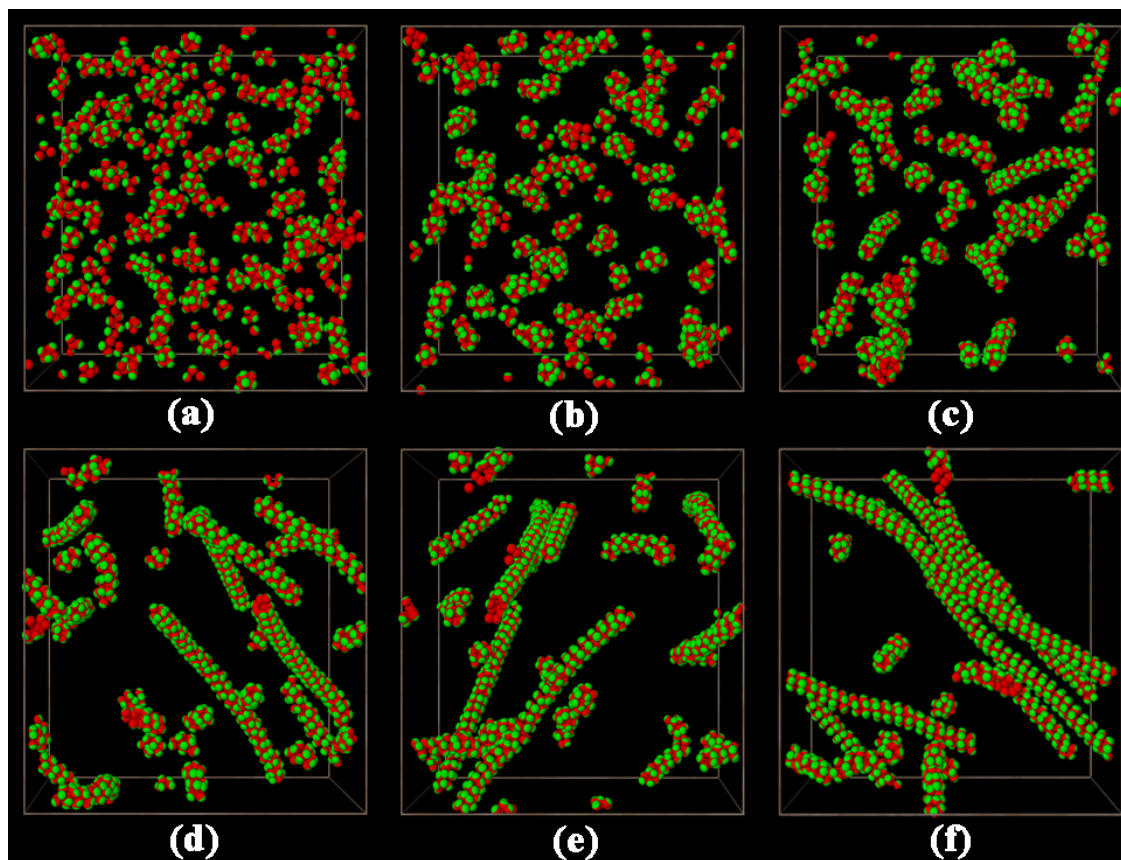


Figure S14: Snapshots taken from the formation process of single helices marked by star symbol e in Fig. 2a, after (a) 140, (b) 700, (c) 2800, (d) 7000, (e) 8400, (f) 16800 time units of simulation.